New Phase Diagram of Oxygen at High Pressures and Temperatures

Mario Santoro,[1,2] Eugene Gregoryanz,[1] Ho-kwang Mao,[1] and Russell J. Hemley[1]

[1]*Geophysical Laboratory, Carnegie Institution of Washington, 5251 Broad Branch Road N.W., Washington, D.C. 20015 USA*
[2]*LENS, European Laboratory for Non-linear Spectroscopy and INFM, Via Carrara 1, I-50019 Sesto Fiorentino, Firenze, Italy*

In situ high P-T Raman measurements and optical observations of solid and fluid oxygen up to 1250 K between 8 and 25 GPa reveal the existence of a new molecular phase η and strikingly unusual behavior of the melting curve. Three triple points were also identified in the P-T domain of the new phase. The data give a direct measure of the melting curve that greatly extends previous optical investigations. We find the melting temperature is significantly higher than that indicated by the existing phase diagram (e.g., 400 K higher at 25 GPa). Raman measurements in low and high frequency regions reveal the extent of orientational order disorder and persistence of strong intermolecular interactions in the high P-T phases.

The profound changes in simple molecular systems induced at high pressures and temperatures are fundamental to a broad range of problems in physics, chemistry, and planetary science [1,2]. Among these molecular materials, oxygen is particularly important. Oxygen has unique features by virtue of its spin ($S = 1$), and the resultant spin-spin interactions affect its numerous P-T phases, making the system a critical test of condensed-matter theory [3,4]. Oxygen is also the third most abundant element in the solar system, and its behavior under extreme P-T conditions provides important insight into the corresponding transitions in other systems such as hydrogen. Furthermore, under high P-T conditions oxygen is a highly reactive material (particularly in the fluid state) and plays a key role in chemical reactions that occur in planetary interiors. Despite the importance of oxygen under extreme conditions, there is a lack of direct experimental information on the system. High P-T shock-wave experiments on oxygen have been limited, and the comparison with theory controversial [5–7]. Static compression experiments, in principle, provide essential information on the equilibrium phase diagram and a range of other physical properties under the required conditions. However, technical problems are thought to preclude *in situ* measurements of oxygen under static pressures and temperatures [8]. Here we report direct measurements of the phase diagram of oxygen over a broad range using new high P-T techniques. We find an unexpected steep increase in the melting temperature with pressure arising from the existence of an altogether new high P-T phase. The significantly higher melting temperature and new phase of oxygen have important implications for the interpretation of dynamic compression experiments as well as for planetary science and first-principles theory.

Oxygen exhibits a rich polymorphism and unusual physical properties [3,4]. Three different solid phases are encountered from 5.5 to 96 GPa, which are all characterized by a layered structure with oxygen molecules perpendicular to a crystal plane and parallel within the layer [9].

In order of increasing pressure, these are the β ($R\bar{3}m$) and δ ($Fmmm$) [10], and the ϵ ($A2/m$) [11] phases. The ϵ phase appears to have a broad pressure domain of stability (up to 86 GPa) and a deep red color arising from strong charge transfer [12]; it was suggested that this phase is made of diamagnetic O_4 molecular units [13–15]. At higher pressure (ζ phase, above 96 GPa) the material is a molecular metal and superconductor [10,16–19]. The extent to which these properties persist at high pressures and temperatures is currently of major interest.

Shock-wave studies performed in the 18–200 GPa and 3000–6000 K range have been confined to the fluid state [5,6]. Within this range, a nonmetal-metal transition was recently reported at 4500 K and 120 GPa and was interpreted as a Mott transition where density-driven band closure and disorder play a fundamental role [5]. First-principles calculations predict a molecular dissociation within the metallic phase and indicate a key role of spin fluctuations in determining the structure of the fluid [7]. On the other hand, shock-wave measurements are limited because pressure and temperature are coupled in a transient experiment, and for oxygen the only probes so far have been electrical conductivity, which does not provide insight about structural and dynamical properties; also, there are concerns about possible chemical reactions of the electrodes used. Static high P-T studies of solid oxygen have been performed in diamond anvil cells only up to 650 K and 16.7 GPa [8,20]. The melting line, solid-solid phase transitions, and the β-δ-ϵ triple point were determined up to 460 K from shifts in the Raman vibron [20]; at higher temperatures only visual observations were employed and on the basis of these observations the existence of the fluid-β-ϵ triple point was inferred. Extending these studies to more extreme conditions has been problematic. Indeed, it has been argued that it is virtually impossible to confine oxygen in diamond cells at temperatures above 650 K due to reactions with the gasket and anvils, leading to the mechanical instability of the container and consequent loss of sample [8].

Recent high P-T experiments on challenging materials such as hydrogen [21] have shown that the use of pure Re as the bulk of the gasket material and very careful execution of the experiment allow temperatures in access of 1100 K to be achieved [21,22]. The oxygen samples were loaded cryogenically through a cold trap in a sealed cylinder. No sign of impurities (e.g., N_2 or CO_2) was found by direct careful Raman measurements at low pressures. Raman spectra were measured with the 488.0 nm Ar-ion laser line. Laser power on the sample was kept within a few tens of mW in order to prevent temperature inhomogeneities due to direct laser heating of oxygen, which easily occurs because of the color. The pressures were determined from *in situ* fluorescence measurements of ruby and Sm:YAG chips loaded in the sample chamber. In order to avoid any errors caused by the movement of the spectrometer grating, in some runs measurements were done with the grating at fixed position during P-T cycles. The measurements of pressure were done by observing the lines of Sm:YAG recorded simultaneously with the vibrational bands. The Raman spectra were measured over a wide spectral range (100–5000 cm^{-1}) before and after heating to check if possible chemical reactions between O_2, Re (gasket), and diamond took place. In one of the loadings the sample was kept under pressure for two months and heated more than 50 times with a few scans up to about 1250 K. Temperature scans to 800–900 K were performed in 1–2 h, while above these temperatures the typical time scale was reduced to 10–20 min. We found that oxygen is very stable at high temperatures and no chemical reactions were ever observed. Phase transitions were detected by crossing the phase boundaries at high temperatures both along isothermal and isobaric P-T paths. The reversibility of the phase transitions was also checked.

Figure 1 shows selected *in situ* high P-T Raman spectra of oxygen. The spectra were collected along approximate isobaric heating runs (16.5–17.7 GPa); at maximum temperature (740 K), the pressure was decreased in order to melt the solid, and the spectrum at 15.2 GPa was measured in the fluid phase. At 580 K the peak of the ϵ phase was observed. A new peak shifted to higher frequencies by about 11 cm^{-1} appears with increasing temperature; this peak is indicative of a phase transition; it was observed in the whole 11.5–19.7 GPa pressure range and was ascribed, depending on pressure, either to β or to a new solid phase, which we call η-O_2 here. At 600 K the coexistence of ϵ and η phases was observed, and the transition to the η phase is complete at 650 K. The melting strongly affects the spectral line shapes: an abrupt broadening was observed and the first hot vibrational band ($\nu = 1$ to 2) appears as a shoulder on the low frequency side of the main peak (see the inset). The FWHM of the peak increases from 4.0 cm^{-1} in the solid to 6.9 cm^{-1} in the fluid [Fig. 1(a)]. The inset shows the spectrum of the vibrational mode in the fluid phase at two different P-T points close to the η and ϵ melting lines, respectively (see Fig. 3). A broad section of the background is shown to emphasize the peak
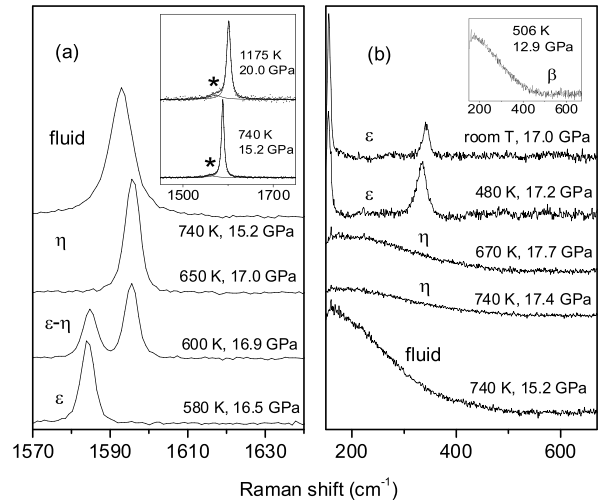

FIG. 1. Raman spectra of oxygen showing the transformation between ϵ and η and fluid phases, between 300 and 740 K, and between 15.2 and 17.7 GPa: (a) vibrational modes in ϵ, η, and fluid phases, (b) lattice modes in ϵ, η, and β (inset) and density of states in fluid. Inset (a): first vibrational hot band of O_2 ($\nu = 1$ to 2) in the fluid state at two temperatures, labeled by asterisks. Two different runs were selected here for presenting the high and the low frequency regions of the spectrum.

asymmetry in the fluid phase, which is related to the hot band. We fitted two Lorentzian line shapes to this asymmetric band, having frequency difference of 27–29 cm^{-1}, which indeed is close to the gas phase anharmonicity (24 cm^{-1}) thus confirming our assignment.

Spectral differences between the phases are also revealed in the lattice modes [Fig. 1(b)]. At room temperature and 480 K the two intense peaks of the ϵ phase are observed at about 155 and 335–342 cm^{-1}, respectively. In the η phase (at 670 and 740 K in the figure) a totally different spectrum is observed; this frequency region is dominated by a very broad band with a shallow maximum around 200 cm^{-1}, which is indicative of orientational disorder. A similar broad band is observed both in the fluid and β phases (inset), where the center of mass of the entire feature is shifted to lower frequencies.

The different phases were also observed optically and provided qualitative evidence of phase transitions. The ϵ phase was characterized by a few crystals, having sizes of 10–30 μm, of pale orange or dark red color depending on orientation and pressure. On forming the β (η) phases from the ϵ phase, grains tend to enlarge into just one or two crystals pinkish (orange) in color. The overall Raman spectrum of the η phase is quite similar to that of β-O_2, but the two phases can be distinguished by quantitative analysis. The vibron frequency difference $\Delta\nu_{\beta(\eta)-\epsilon}$ was measured at the phase coexistence between β and ϵ and between η and ϵ phases [Fig. 2(a)]. In both cases β (η) was reached from the ϵ phase, by either increasing T or decreasing P. The quantity $\Delta\nu_{\beta(\eta)-\epsilon}$ shows a jump of about 1.6 cm^{-1} and a slope change at 15.7 (±0.2) GPa and

temperature 540 ($\pm$20) K. This result shows the phase transition between β and η phases, and the discontinuity in $\Delta\nu_{\beta(\eta)-\epsilon}$ versus pressure represents the triple point (see Fig. 3, point A) between β, η, and ϵ phases. In order to confirm the triple point we also investigated the surrounding area of the phase diagram by doing isothermal pressure scans at slightly lower and higher temperatures; two selected scans are reported in Figs. 2(b) and 2(c) where the pressure shift of the vibrational frequency is plotted. At 511 K (i.e., below the triple point) the frequency increases linearly with pressure in the β phase up to the onset of the β-ϵ phase transition, occurring at 14.9 ($\pm$ 0.1) GPa, and the two points above this pressure were collected at the phase coexistence; i.e., at this temperature we do not have evidence of other phases, prior the onset of the ϵ phase, other than β-O_2. On the other hand, above the triple point at 589 K, the frequency undergoes a slope change and a very small jump of 0.2 cm^{-1} at 15.6 ($\pm$ 0.1) GPa, showing the β-η phase transition; at 16.5 ($\pm$ 0.1) GPa η-O_2 transforms to the ϵ phase.

Our findings lead to a new P-T phase diagram of oxygen (Fig. 3). The previous phase diagram (cited throughout the literature, e.g., Refs. [3,4,23]) is also shown. Our β phase melting data are in good agreement with previous results
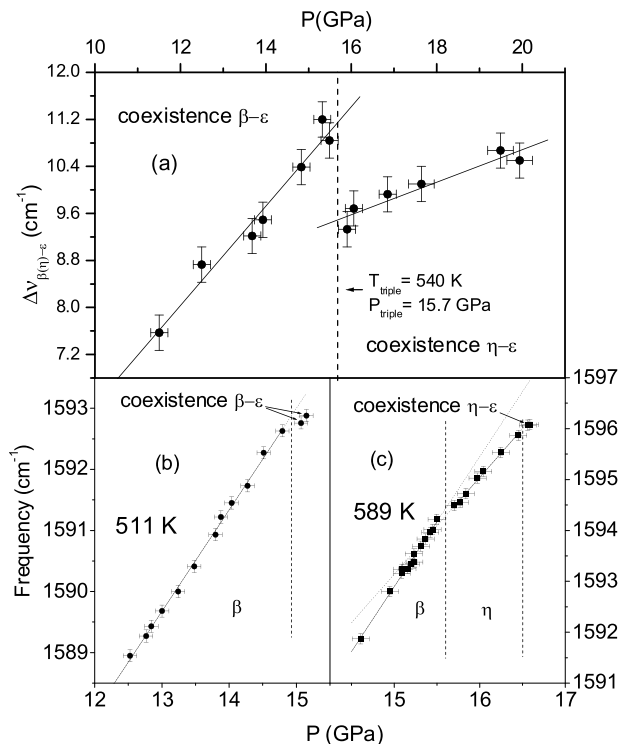
[8,20] up to 15.0–15.5 GPa and about 620 K. Beyond this range the slope of the melting line sharply increases. At higher P-T it changes again and a new sharp kink appears around 20 GPa and 1050 K. These observations alone clearly reveal the existence of the new η phase. As far the solid-solid phase transitions are concerned, we found that the phase boundary between β and ϵ oxygen is in good agreement with previous data [20] up to about 12.5 GPa; then it shifts to higher pressures, and the shift increases with temperature. The η-ϵ phase boundary was detected up to about 19.7 GPa and 920 K, and we note that its slope steeply increases with pressure. A transition point between pure β-O_2 and η-O_2, detected along isothermal pressure scans [Fig. 2(c)], was also found. Melting data points were fitted by polynomials. Polynomial fits of the data were also used to obtain the β-ϵ, β-η, and η-ϵ transition lines. The intersections of the new phase transition boundaries provide evidence of the β-η-fluid (point B) and η-ϵ-fluid (point C) triple points positioned at 15.6 ($\pm$ 0.2) GPa and 624 ($\pm$ 20) K, and at 20.0 ($\pm$ 0.4) GPa and 1050 ($\pm$ 40) K, respectively. We point out that the fitting lines were obtained taking into account the thermodynamic constraints implied by the phase rule; i.e., we allowed each of the phases lying around a triple point to contain only one metastable extension of the phase boundaries falling into each phase field.

Raman data provide important information concerning the structure of η-O_2. The symmetry of this phase is expected to be closely related to that of β-O_2, since the

FIG. 2. Frequency difference $\Delta\nu_{\beta(\eta)-\epsilon}$ between the vibron Raman peak of β (η) and that of the ϵ phase as a function of pressure at different temperatures, measured along the phase coexistence between $\beta(\eta)$ and ϵ phases (a); frequencies of vibron as a function of pressure in the β (b) and between the β and η phases (c), up to the onset of the ϵ phase. The temperature was kept constant within one to two degrees along the isothermal scans (b),(c).
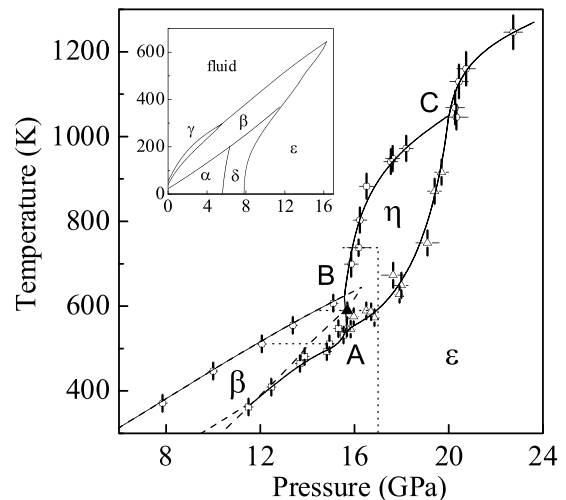

FIG. 3. Extended phase diagram of oxygen. The dashed lines represent the previous phase diagram reviewed in Refs. [3,4,23] which in turn is replotted by continuous lines in the inset. The dots are data obtained in this work: melting points (open circles), β-ϵ (open squares), η-ϵ (open triangles), and β-η (full triangles) phase transition points, respectively. A, B, and C label triple points (see the text). Errors bars involve single measurement uncertainties and those related to the determination of the onset of the phase transitions. Dotted lines: P-T trajectories corresponding to the approximate paths shown in Figs. 1, 2(b), and 2(c).

spectra of the two phases are similar. The η phase is orientationally disordered as indicated by the lattice region spectrum. The corresponding spectrum of β-O_2 was previously observed only at low temperature (below 220 K) [24], where a single phonon peak was reported, despite long range disorder in the stacking of crystal planes [25]. This result, together with our findings, points to a progressive temperature-induced disorder in β-O_2. The β-η phase transition appears first order, and a negative ΔV of transformation is expected; on the other hand, this reduction would be smaller than that experienced at the β-ϵ transition ($\sim 10\%$) since the frequency shift is much smaller. In addition, an increased amount of charge transfer is expected in η-O_2 than in β-O_2, because of the stronger optical absorption.

One of the most unexpected aspects of the new P-T phase diagram is the steep melting line of the η phase close to triple point B, which implies that the entropy of η-O_2 approaches the entropy of the fluid phase value close to this point, and that η-O_2 is more entropic than β-O_2; the latter is likely due to increased orientational disorder in the η phase. The melting line of the ϵ phase and the $\eta - \epsilon$ phase boundary near triple point C are also very steep. This can be ascribed to the high density of ϵ oxygen and to the expected charge transfer related disorder of this phase. The high frequency shift of the internal mode peak was observed in transforming the sample from higher to lower density phases (a part of β-fluid phase transition); the shift is from 0.2 to 11 cm^{-1} depending on phase transitions, pressure, and temperature. This behavior points out that the shift is mainly due to the charge-transfer effects that increase with density. Charge transfer tends to lower the internal molecular frequency by transferring the electronic charge from the intramolecular to intermolecular regions. Finally we point out that among the three high-temperature solid phases, β, η, and ϵ oxygen, the last is the only one where well-defined phonon peaks were observed up to melting. This result shows the qualitatively different orientational nature of oxygen in ϵ compared to β and η phases. Strong intermolecular interactions between O_2 molecules (O_4 clusters) in which the librational modes of the constituent O_2 units merge into internal modes of the cluster [13,14] could explain the persistence of the ''phonon'' peaks up to very high temperature.

In summary, direct measurements of the phase diagram of oxygen over an extended P-T range reveal a sharp rise in the melting temperature above 15.6 GPa arising from the existence of a new high-temperature phase, η-O_2. This change in the topology of the phase diagram should be taken into account in the interpretation of shock-wave experiments. The results are also important for characterizing the state and thermochemical properties in planetary interiors. The new high P-T phase is shown to be orientationally disordered with a high degree of charge transfer; also, the β phase was found to undergo a progressive temperature-induced orientational disorder. These results also provide stringent tests of theoretical calculations of the high P-T behavior of oxygen, which remains challenging because of the presence of molecular spins.

[1] R. J. Hemley, Annu. Rev. Phys. Chem. **51**, 763 (2000).
[2] V. Schettino and R. Bini, Phys. Chem. Chem. Phys. **5**, 1951 (2003).
[3] D. A. Young, *Phase Diagrams of the Elements* (University of California Press, Oxford, England, 1991).
[4] Y. A. Freiman and H. J. Jodl, Phys. Rep. **401**, 1 (2004).
[5] M. Bastea, A. C. Mitchell, and W. J. Nellis, Phys. Rev. Lett. **86**, 3108 (2001).
[6] D. C. Hamilton et al., J. Chem. Phys. **88**, 5042 (1988).
[7] B. Militzer, F. Gygi, and G. Galli, Phys. Rev. Lett. **91**, 265503 (2003).
[8] D. A. Young et al., Phys. Rev. B **35**, 5353 (1987).
[9] M. Nicol and K. Syassen, Phys. Rev. B **28**, 1201 (1983).
[10] S. Desgreniers, Y. K. Vohra, and A. L. Ruoff, J. Phys. Chem. **94**, 1117 (1990).
[11] B. Olinger, R. L. Mills, and R. B. Roof, Jr., J. Chem. Phys. **81**, 5068 (1984); S. W. Johnson, M. Nicol, and D. Schiferl, J. Appl. Crystallogr. **26**, 320 (1993); S. Desgreniers and K. Brister, in *High Pressure Science and Technology*, edited by W. A. Trzeciakowski (World Scientific, Singapore, 1996), p. 363.
[12] M. Nicol, K. R. Hirsch, and W. B. Holzapfel, Chem. Phys. Lett. **68**, 49 (1979).
[13] F. Gorelli, L. Ulivi, M. Santoro, and R. Bini, Phys. Rev. Lett. **83**, 4093 (1999).
[14] F. Gorelli, L. Ulivi, M. Santoro, and R. Bini, Phys. Rev. B **63**, 104110 (2001).
[15] M. Santoro et al., Phys. Rev. B **64**, 064428 (2001).
[16] K. Shimizu et al., Nature (London) **393**, 767 (1998).
[17] Y. Akahama et al., Phys. Rev. Lett. **74**, 4690 (1995).
[18] G. Weck, P. Loubeyre, and R. LeToullec, Phys. Rev. Lett. **88**, 035504 (2002).
[19] A. F. Goncharov, E. Gregoryanz, R. J. Hemley, and H. K. Mao, Phys. Rev. B **68**, 100102 (2003).
[20] J. Yen and M. Nicol, J. Phys. Chem. **91**, 3336 (1987).
[21] E. Gregoryanz et al., Phys. Rev. Lett. **90**, 175701 (2003).
[22] E. Gregoryanz et al., Phys. Rev. B **66**, 224108 (2002).
[23] F.A. Gorelli and M. Santoro, J. Raman Spectrosc. **34**, 549 (2003).
[24] H. Jodl, F. Bolduan, and H. Hochheimer, Phys. Rev. B **31**, 7376 (1985).
[25] H. d'Amour, W. B. Holzapfel, and M. Nicol, J. Phys. Chem. **85**, 130 (1981).